Impurities in Hydride Gases Part 2: Investigation of Trace CO_2 in the Liquid and Vapor Phases of Ultra-Pure Ammonia

HANS H. FUNKE,[1] JON WELCHHANS,[1] TADAHARU WATANABE,[1] ROBERT TORRES,[1] VIRGINIA H. HOULDING,[1] and MARK W. RAYNOR[1,2]

1.—Matheson Tri-Gas, Inc., Advanced Technology Center, Longmont, CO 80501. 2.—E-mail: mraynor@matheson-trigas.com

Ammonia (NH_3) as a precursor for epitaxial nitride films is required to be free of trace oxygenated impurities, such as CO_2, that have been shown to negatively affect growth processes and device performance. Carbon dioxide can react reversibly with the NH_3 gas to form ammonium carbamate, NH_4COONH_2 (a solid with low solubility in liquid NH_3) and, therefore, can be present in cylinder sources both in the free and chemically bound form. A gas chromatograph (GC)-based method has been developed to accurately quantify the total CO_2 content in both vapor- and liquid-phase NH_3 streams. A heated GC-sampling manifold is used to thermally decompose any NH_4COONH_2 present in the sample or calibration standard so that all CO_2 is analyzed in its free form. Several commercial cylinder sources maintained at room temperature were analyzed by this method, and in all cases, equilibrium concentrations of <75 parts-per-billion by volume (ppbv) CO_2 were present in the gas phase as long as residual liquid was present. Slightly higher concentrations were found in the liquid phase, and upon exhaustion of the liquid phase and heating, CO_2 levels strongly increased to parts-per-million by volume (ppmv) levels. The excess CO_2 is likely adsorbed on the cylinder walls or dispersed in the liquid as solid NH_4COONH_2. These results are consistent with thermodynamic calculations based on equilibrium data for the carbamate system available in the literature. To meet the purity requirements of organo-metallic vapor-phase epitaxy processes, the performance of an adsorbent-based purifier that is capable of removing residual CO_2 in both free and chemically bound forms from NH_3 streams is discussed.

Key words: Carbon dioxide, impurities, ammonia, ammonium carbamate, gas chromatography

INTRODUCTION

Minimizing the incorporation of oxygen in GaN and other epilayers during metal-organic chemical-vapor deposition is critical to the performance of high brightness light-emitting diodes and laser devices. Oxygen, which is believed to be a shallow donor,[1] can cause crystal lattice defects that affect optical and electrical properties, such as photoluminescence, optical absorption, thermal conductivity, and Hall mobility.[2–5] Also of concern is carbon, an amphoteric impurity that is predicted to be a shallow acceptor in (Al)GaN and can result in donor compensation and yellow luminescence commonly observed in GaN.[1]

Even though trace oxygenated impurities may be introduced from a number of sources, such as the carrier and purge gases or from the organo-metallic precursors,[6–8] the ammonia (NH_3) process gas can be a significant source of oxygen contamination from impurities, such as moisture and carbon dioxide. In the case of carbon dioxide, unintentional carbon incorporation during film growth also cannot be ruled out. It is, therefore, important to develop sensitive detection methods for the key impurities to understand the physical behavior of the contamination

(Received July 13, 2003; accepted January 15, 2004)

sources and to ultimately minimize the concentration of these impurities for improved process control. Even if appropriate analytical techniques are available, however, trace contaminants are often difficult to accurately quantify in liquefied gas sources because of partitioning into the liquid phase[9] and/or their tendency to form reaction products with the reactive source gas.

In the first part of this series, the thermodynamic behavior of trace moisture impurities in liquefied NH_3 was studied experimentally using Fourier-transform infrared spectroscopy.[10] Moisture was found to dissolve readily in liquid NH_3. Gas-phase sampling from wet NH_3 sources resulted in strongly fluctuating moisture concentrations caused by equilibrium shifts, boiling processes, and enrichment of the less volatile moisture as the sources were consumed. More accurate information about the true moisture content in the cylinder was obtained by continuously sampling from the liquid phase and vaporizing the sample prior to analysis. The system could be qualitatively described by a two-component vapor/liquid equilibrium approach.

In addition to partitioning effects, it is important to consider that oxygenated impurities can chemically react with Group V hydride gases to form insoluble or only partially soluble reaction products. Introduction of trace atmospheric oxygen into arsine and phosphine, for example, is known to result in the formation of oxides and oxy-acids that escape detection by standard analytical approaches monitoring for free oxygen impurities only.[11] Furthermore, as chemical reactions can be reversible, gaseous impurity levels that are detected may vary depending on analysis or gas usage conditions that affect the reaction equilibrium.

This work attempts to complement the conclusions from the moisture studies by investigating the properties of carbon dioxide traces in liquid NH_3 as a model system for an impurity that can reversibly react with the source gas. A new analytical sampling procedure is reported for reliable detection of CO_2 in NH_3, and a thermodynamic model that describes the behavior of this system is discussed. Finally, the performance of an adsorbent-based purifier for efficiently removing trace CO_2 in gaseous NH_3 streams is presented.

REACTION CHEMISTRY

The reaction of NH_3 with CO_2 has been studied extensively because of the commercial importance for urea synthesis.[12–15] The NH_3 reacts in a first reversible step with CO_2 to form ammonium carbamate (NH_4COONH_2), a white crystalline solid (molecular weight = 78 g/mol) according to Eq. 1:

$$2\ NH_3 + CO_2 \rightleftharpoons NH_4COONH_2 \qquad (1)$$

This reaction is exothermic with a heat of dissociation of ~159 kJ/mol.[15] Upon heating above ~100°C, NH_4COONH_2 slowly decomposes by releasing water to form urea according to

$$NH_4COONH_2 \rightarrow NH_2CONH_2 + H_2O \qquad (2)$$

The enthalpy of endothermic reaction 2 is ~31.4 kJ/mol.[16] The equilibrium concentration of urea is negligible at ambient temperature[13,17] but approaches >80% at temperatures above 150°C.[18] Another side reaction is the reversible formation of ammonium carbonate in the presence of water that is shifted to the precursors above ~60°C:

$$NH_4COONH_2 + H_2O \rightleftharpoons (NH_4)_2CO_3 \qquad (3)$$

Of primary interest for the measurement of trace CO_2 contamination in liquefied NH_3 sources is the first reaction step that determines the concentration of free CO_2 in the cylinder headspace and precipitation of excess CO_2 as solid NH_4COONH_2 dispersed in the liquid reservoir or adsorbed on the cylinder walls.

EXPERIMENTAL APPROACH

Analytical Instrumentation and Sampling Manifold

A new method based on gas chromatography with a pulsed-discharge ionization detector (GC-PDID) was developed to quantify trace CO_2 in NH_3 at the low parts-per-billion by volume (ppbv) levels. A Shimadzu GC-14A GC (Kyoto, Japan) equipped with a PDID (Valco Instruments, Houston, TX), a heated switching valve oven, and two porous-polymer 6′ × 2-mm inner diameter packed columns were used for all measurements. Figure 1 illustrates the column setup with a standard back-flush configuration to prevent the analyte gas from entering the detector. All lines were heated above 60°C to minimize the formation of solid NH_4COONH_2, according to Eq. 1, and shift the equilibrium toward the reactants. A schematic of the sampling manifold including temperature-controlled zones to calibrate the instrument, optimize the CO_2 response, and perform purifier investigations is shown in Fig. 2.

Without heating of the lines, as much as 50% of the CO_2 added to the gas stream is lost because of

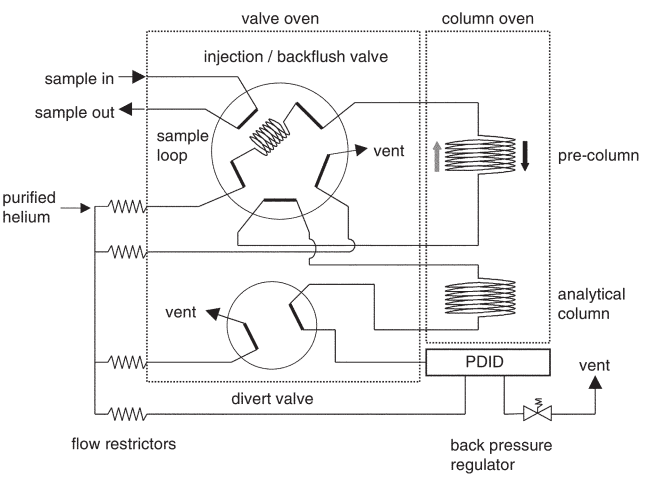

Fig. 1. Schematic diagram of the GC-PDID system.

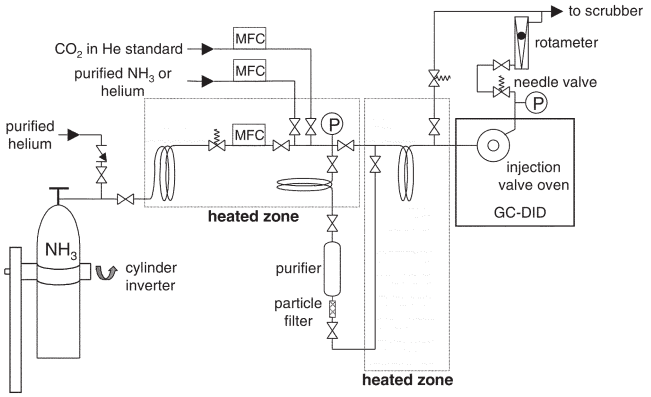

Fig. 2. Sampling manifold with two independently heated zones for calibration, liquid- and vapor-phase sampling of NH_3 cylinders, and purifier evaluations.

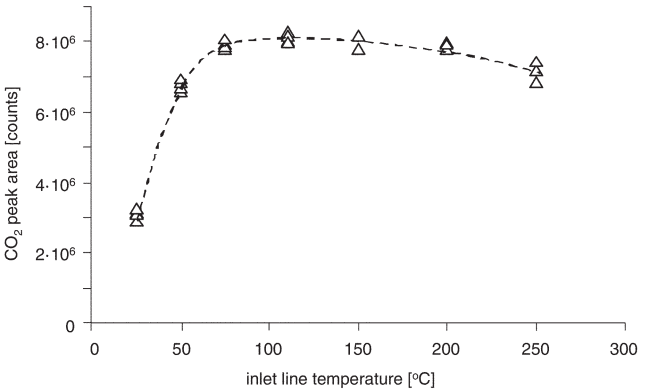

Fig. 3. Effect of manifold temperature on GC response to 90-ppmv CO_2 added to purified NH_3.

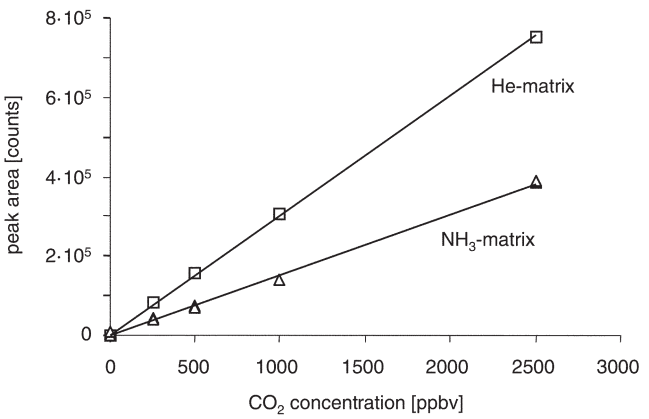

Fig. 4. Calibration curves for CO_2 in He (□) and NH_3 (△) matrices.

NH_4COONH_2 formation,[19] indicating that trace CO_2 exists simultaneously in both free and chemically bound forms in NH_3 depending on the temperature of the sampling system. The effect of sampling manifold temperature on free CO_2 response was investigated by heating both zones 1 and 2 in Fig. 2 in the range from 30°C to 250°C and analyzing NH_3 spiked with 90 ppmv CO_2. As shown in Fig. 3, the CO_2 response increased with increasing line temperature, and after reaching a maximum near 110°C, started to decrease as the temperature was raised further. The decreased response above 110°C is likely due to the formation of urea according to Eq. 2 that is favored at higher temperatures. All cylinder measurements were performed at line temperatures of 110°C to maximize sensitivity.

Calibration and Data Analysis

A comparison of calibration curves obtained in NH_3 and He (Fig. 4) indicates that even at optimized conditions, the detector response in NH_3 is only about 50% of the response in He. This discrepancy may be due to (1) incomplete decomposition of the NH_4COONH_2 in the heated lines and manifold; (2) the occurrence of other side reactions, such as urea formation; or (3) reduced instrument sensitivity caused by NH_3. The limit of detection for CO_2 in NH_3 calculated from 3 signal/noise[20] was 11 ppbv. Using the more stringent International Union of Pure and Applied Chemistry definition based on 3 σ/m (σ = standard deviation of peak area fluctuations; m = slope of calibration curve),[21] the limit of detection was 30 ppbv. All cylinder data presented are based on calibrations performed in NH_3 and care was taken to prevent exposure of the sample stream to temperatures above 110°C to avoid urea formation.

Partitioning of CO_2 in the Gas and Liquid Phases

The measurement of CO_2 concentrations in the liquid and gas phases of liquefied NH_3 cylinder sources at different total CO_2 contents provides information about the validity of the previously discussed reaction equilibrium. The gas-phase concentration directly reflects the equilibrium vapor pressure, whereas liquid concentrations could be due to either dissolved NH_4COONH_2 or dispersed particles entering the sampling system.

Liquid Sampling Procedure

Cylinders were inverted using a custom valve jacket or a cylinder inverter for sampling of the liquid phase. The liquid withdrawn in the inverted orientation was completely vaporized in a heated line segment at a temperature of ~110°C.[10] The pressure in the heated line segment was determined by the vapor pressure of the liquid in the cylinder at ambient temperature (~8.5 atm), and the flow rate was controlled by a mass flow controller.

CO_2 Addition to Cylinder Source

Small amounts of CO_2 were added into a cylinder containing ~4-kg high-purity liquid NH_3, by pressurizing a 5-cc sample line connected to the cylinder valve with CO_2, to a pressure of ~5 atm above cylinder pressure. By briefly opening the cylinder valve to avoid NH_3 back-diffusion, the CO_2 expanded into the cylinder until cylinder pressure was reached. Added CO_2 concentrations were calculated using the ideal gas law. The cylinder was inverted and

rolled several times after each CO_2 addition and stored overnight to re-equilibrate before sampling was initiated.

Mixing of CO_2 and NH_3 Streams

A glass vessel was equipped with two inlet lines and a vent line to determine the ease of NH_4COONH_2 formation at ambient conditions by visible observation. Prior to introducing the reactant gases, the vessel was purged with dry N_2 and heated with a heat gun to minimize residual moisture.

Purifier Testing

A 60-cm^3 stainless steel vessel was filled in a dry N_2 purged glove box with a Nanochem® NHX purifier material (Matheson Tri-Gas, Inc., Longmont, CO) and equipped with a 0.003-μm particle filter at the outlet. Impurity challenges for the measurement of purifier efficiency were obtained by mixing CO_2 standard gas with NH_3 using mass flow controllers (Fig. 2). For purifier capacity measurements, the CO_2 challenge was supplied in He carrier gas because the formation of NH_4COONH_2 results in blockage of the unheated purifier vessel at concentrations of ~500-ppmv CO_2 that are necessary to saturate the purifier within a reasonable time frame.

RESULTS AND DISCUSSION

NH_4COONH_2 Formation

By adding CO_2 to a dry NH_3 stream at ambient conditions inside a dry glass container, qualitative observations of NH_4COONH_2 formation were possible. As shown by the photographs in Fig. 5, the formation of a white cloud was visible at the mixing point of the two gas streams a few seconds after the CO_2 gas stream was initiated. The glass surface and the ends of the gas lines, however, were quickly coated with a white film that could be removed by heating the vessel with a heat gun. The film was assumed to be NH_4COONH_2, but a fraction of ammonium carbonate from reaction with residual moisture (Eq. 3) on the glass wall could not be ruled out completely.

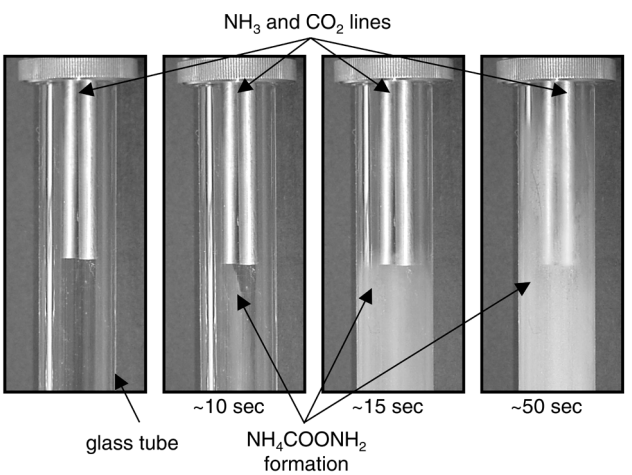

Fig. 5. Photograph of ammonium carbamate (NH_4COONH_2) film formed by mixing 25-sccm CO_2 and 100-sccm NH_3 streams inside a glass tube at ambient pressure and temperature.

The kinetics of formation of NH_4COONH_2 from NH_3 and CO_2 has not been studied widely, and results are controversial.[22–24] Solid surfaces appear to play an important role for nucleation even though the experimentally observed cloud formation indicates the possibility of gas-phase reactions or nucleation on dust particles in the gas stream. Traces of moisture are believed to facilitate the reaction because both NH_3 and CO_2 are more readily adsorbed on moist surfaces.[22] The rate of reaction increases with decreasing temperature, and equilibrium is typically established a few minutes after an induction period that depends on the affinity of the reaction surfaces for adsorption of the precursors. Reaction in the condensed liquid phase also cannot be ruled out.[22] The impact on a large excess of one of the precursors, such as in liquefied NH_3 cylinders, has not been discussed by the cited sources.

One of the questions that arise from the preceding assumptions about the kinetic mechanisms is the location of the precipitated solid. In a liquefied gas source, the solid could either be dispersed more or less finely in the liquid or attached to the cylinder walls above or below the liquid level. Depending on the adhesion strength to the wall, agitation of the cylinder content might dislocate attached carbamate particles into the liquid. As surface tension of small particles is large, and assuming a finite solubility, dispersed particles might also slowly dissolve in the liquid and reprecipitate on the cylinder wall.

Cylinder Analysis

Liquid- and gas-phase NH_3 from different cylinder sources was analyzed using heated sampling lines to evaluate the partitioning of CO_2 between the two phases. Table I lists the results for nine different cylinders. The CO_2 concentrations reported are based on an average of five GC analyses. In full cylinders, CO_2 concentrations in the gas phase were $<$75 ppbv and remained in this range as gaseous NH_3 continued to be withdrawn from the cylinder.

Liquid-phase CO_2 levels were similar or only slightly higher than gas-phase concentrations,

Table I. CO_2 Concentration in the Gas and Liquid Phases of NH_3 Cylinders*

Cylinder	Gas Phase CO_2 (ppbv)	Liquid Phase CO_2 (ppbv)
1 (full)	22 ± 4	48 ± 2
2 (full)	18 ± 6	23 ± 14
3 (full)	27 ± 4	58 ± 10
4 (full)	58 ± 7	59 ± 7
5 (full)	47 ± 4	NA
6 (full)	NA	207 ± 40
7 (full)	61 ± 4	91 ± 9
8 (full)	30 ± 4	40 ± 3
9 (370 g)	22 ± 19	921 ± 684

*Analysis uses heated lines at 110°C.

except for cylinder 9 as the liquid phase was close to being depleted. With about 370-g residual liquid phase, CO_2 concentrations in the liquid phase were strongly fluctuating at ~1 ppmv, suggesting that loose NH_4COONH_2 or ammonium carbamate-coated rust particles were entering the sampling system. The gas-phase concentrations remained at ~22 ppbv in the depleted cylinder 9 while the liquid phase was present.

After all liquid was evaporated, CO_2 concentrations typically increased strongly as sampling of the residual gas-phase NH_3 was continued. Heating the cylinder walls further magnified this effect as the dissociation equilibrium in Eq. 1 was shifted from solid NH_4COONH_2 to the reactants.

Cylinder 3, for example, which originally contained 27-ppbv CO_2 in the gas phase and 58-ppbv CO_2 in the liquid phase when full, was later found to contain 0.5-ppmv CO_2 when liquid dry (cylinder conditions: 4 atm and 22°C). As shown in Fig. 6, the CO_2 concentration increased significantly as the cylinder temperature increased. A concentration of 9.8-ppmv CO_2 was measured as the cylinder temperature reached ~101°C. The remaining high concentration observed after decreasing the cylinder temperature to 68°C is likely due to a lack of equilibration time and limited sample flow because the experiments were performed in a continuous run over the course of ~5 h. By integrating the data in Fig. 6 and assuming that at 101°C the majority of NH_4COONH_2 was decomposed, the amount of residual CO_2 in the cylinder was estimated to be ~0.003 g after the liquid reservoir was exhausted. A content of 3 mg of solid NH_4COONH_2 (size ~20 Å^2) evenly dispersed on the internal surface of a typical cylinder (~0.9 m^2) would result in a layer thickness of only about 6 monolayers.

From the liquid and gas CO_2 concentrations of a full cylinder containing ~22.6-kg NH_3 that typically amounted to ~0.1 ppmv or less, an additional 0.003-g CO_2 were calculated. Because liquid phase concentrations were similar for most cylinders, even though additional CO_2 was present as solid NH_4COONH_2 (Fig. 6), detected concentrations appear to be dictated by the solubility limits of NH_4COONH_2 in liquid NH_3, amounting to a solubility of $\sim 1 \times 10^{-6}$ mol/l.

CO_2 Addition

Because the range of CO_2 concentrations in the cylinders studied was relatively narrow, pure CO_2 was intentionally added to a cylinder containing 4 kg of high-grade NH_3 to study a wider concentration range and to confirm that gas and liquid concentrations are limited by the solubility and NH_4COONH_2 dissociation equilibrium. The liquid- and gas-phase concentrations after consecutive addition of 6.3 ppmv and 32.4 ppmv of CO_2 are shown in Fig. 7 as a function of total calculated CO_2 content in the cylinder. The cylinder was rolled and equilibrated over night after each addition prior to the measurements. Each data point was averaged from five consecutive measurements. The maximum concentrations in the gas phase after addition of 6.3 ppmv were similar to the previously detected levels in several cylinder sources (Table I). After further introducing 26.1 ppmv of CO_2 to the cylinder for a total content of 32.4 ppmv, gas-phase concentrations showed larger fluctuations even though overall concentrations rose only slightly to ~250 ppbv. It appears that all free-added CO_2 precipitates on the cylinder walls according to the carbamate equilibrium or enters the liquid phase. The increase in variance of the measurement might be caused by NH_4COONH_2 particles deposited close to the cylinder valve that are dislocated during sampling. Liquid phase measurements showed a more pronounced increase in CO_2 concentration to ~0.6 ppmv and 1.5 ppmv, respectively. Fluctuations of the data points increased strongly with increasing CO_2 content, which is also very likely due to random sampling of free floating or dislocated NH_4COONH_2 particles.

Heating the cylinder while still containing liquid-phase NH_3 incrementally to 65°C initially caused gas-phase CO_2 concentrations to increase to 2–3 ppmv, but after continued sampling, again decreased to concentrations close to those observed at ambient temperature. These observations are inconsistent

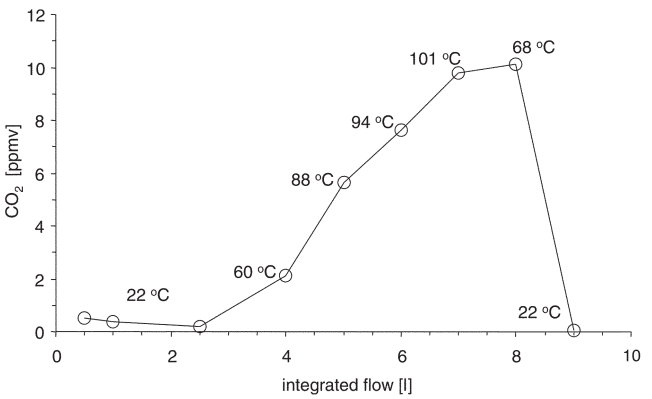

Fig. 6. The CO_2 concentrations of a gas stream withdrawn from a liquid-dry cylinder (Cylinder 3 in Table II) with ~3.7-atm residual NH_3 pressure at different cylinder temperatures.

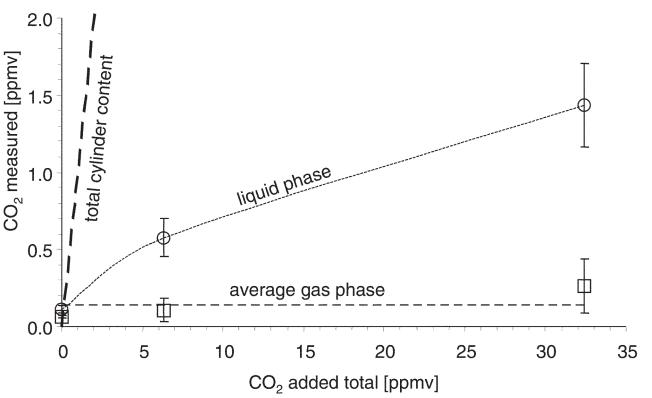

Fig. 7. The CO_2 concentration in the gas and liquid phases of an intentionally doped NH_3 cylinder (□: gas-phase samples, ○: liquid-phase samples).

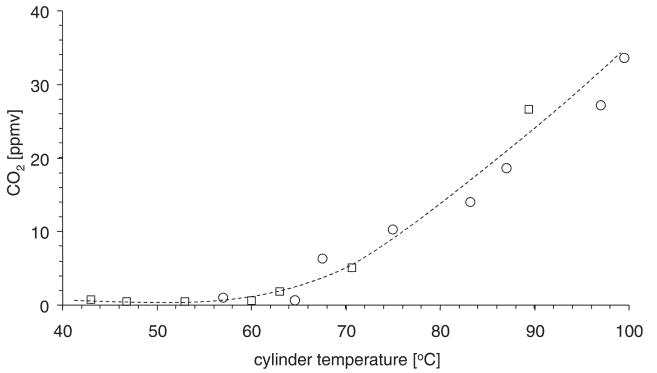

Fig. 8. The CO_2 emissions from a heated liquid-dry cylinder containing 32-ppmv CO_2 prior to exhaustion of the liquid phase (□: first heating cycle, ○: second heating cycle).

with the assumption of the carbamate equilibrium, which favors the precursors at higher temperatures, and other factors have to be considered. Among the possible causes are the increased solubility of NH_4COONH_2 or free CO_2 in the liquid phase, insufficient sampling time because of the large headspace in the cylinder, variation in the cylinder temperature, localized cooling caused by vaporization of NH_3 from the liquid phase, or precipitation of NH_4COONH_2 in cool spots.

After the liquid phase was exhausted and the residual gas-phase pressure reached ~3 atm, the cylinder was incrementally heated to 100°C to qualitatively verify that the added CO_2 that was assumed to be stored as NH_4COONH_2 could be released. In Fig. 8, the results of two heat cycles are shown. Free CO_2 concentrations above 35 ppmv were detected at temperatures approaching 100°C. Calibration data were only collected to ~10 ppmv; higher concentrations were extrapolated using the slope of the calibration curves.

Thermodynamic Predictions

The measured gas-phase concentrations were compared with thermodynamic calculations based on literature data for the $NH_3/CO_2/NH_4COONH_2$ equilibrium. The equilibrium constant K_p for the formation of NH_4COONH_2 (Eq. 1) can be calculated based on the stoichiometry and the formation of a solid reaction product:

$$K_p = p_{NH_3}^2 \, p_{CO_2} \quad (4)$$

The terms p_{NH_3} and p_{CO_2} are the partial pressures of NH_3 and CO_2, respectively, in the gas mixture. Several studies discuss this reaction in detail. Bennet et al.[25] determined K_p between 24°C and 63°C by measuring the stoichiometric dissociation pressure, P_{diss}, of samples of solid NH_4COONH_2:

$$p_{NH_3} = 2 \, p_{CO_2} \quad (5)$$

With $P_{diss} = p_{NH_3} + p_{CO_2}$ at a given temperature, p_{NH_3}, p_{CO_2}, and K_p can be calculated:

$$p_{NH_3} = 2P_{diss}/3 \text{ and } p_{CO_2} = P_{diss}/3 \quad (6)$$

$$Kp = 4P_{diss}^3/27 \quad (7)$$

Similar experiments were also performed by Janjic[26] and equilibrium constants and calculated free energies were comparable. From these data, the maximum concentration of free CO_2 C_{CO_2}(in ppmv) in a cylinder containing liquid NH_3 and an excess of solid NH_4COONH_2 can be estimated with Eq. 4 because the total pressure in the cylinder equals the vapor pressure p_{NH_3} in good approximation:

$$C_{CO_2} = p_{CO_2}/p_{NH_3} \times 10^6 = (K_p/p_{NH_3}^2)/p_{NH_3} \times 10^6 \quad (8)$$

In Table II, results of such estimations for different temperatures are listed. For example, at 20°C, the dissociation pressure P_{diss} = 0.0874 atm.[25] From Eq. 7, an equilibrium constant $K_p = 9.89 \times 10^{-5}$ atm^3 follows. With a vapor pressure for NH_3 of ~8.5 atm at this temperature, the maximum concentration of free CO_2 in the gas phase is about 162 ppbv. Further addition of CO_2 will result in precipitation of solid NH_4COONH_2 without an increase in the gas-phase CO_2 concentration. The predicted concentrations of free CO_2 in the cylinder headspace are similar in magnitude but somewhat higher than the measured data in Table I. Because temperatures inside the cylinder were not controlled during gas withdrawal, evaporative cooling might have caused decreases in the cylinder temperature. As indicated in Table II, decreasing the temperature strongly decreases the equilibrium concentration of free CO_2. Additionally, deviation from the ideal behavior of the equilibrium constant caused by the presence of liquid NH_3, elevated pressure, and low total CO_2 content have to be considered.

Table II. Estimated Concentrations of Free CO_2 in the Headspace of a Cylinder Containing Liquefied NH_3

T (°C)	Dissociation Pressure* P_{diss} (atm)	$K_p = 4 \times P_{diss}^3/27$ K_p (atm)	Vapor Pressure p_{NH_3} (atm)	$C_{CO_2} = (K_p/p_{NH_3}^2)/p_{NH_3} \times 10^6$ C_{CO_2} (ppmv)
0	0.0188	9.84×10^{-7}	4.28	0.013
10	0.0417	1.07×10^{-5}	6.11	0.047
20	0.0874	9.89×10^{-5}	8.49	0.162
24.4	0.1172	2.38×10^{-4}	9.76	0.257
30	0.1744	7.86×10^{-4}	11.55	0.510
40	0.3333	5.49×10^{-3}	15.30	1.532

*From Ref. 25.

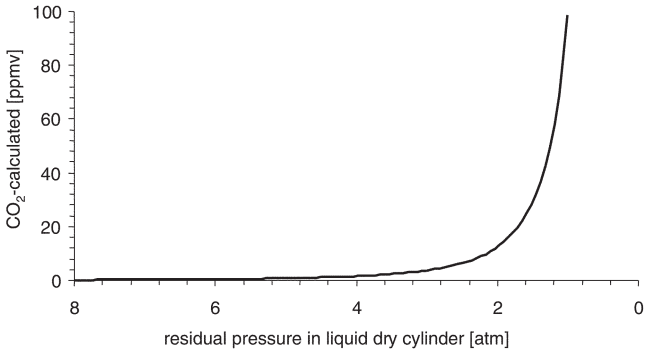

Fig. 9. Calculated CO_2 concentration of NH_3 withdrawn from a liquid-dry cylinder containing solid NH_4COONH_2 at 20°C as the residual gas-phase NH_3 is exhausted.

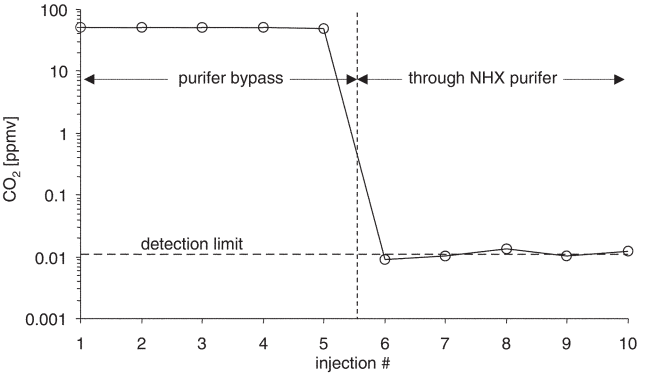

Fig. 10. Efficiency of Nanochem® NHX purifier material for removal of 50-ppmv CO_2 in NH_3 (temperature zones 1 and 2 heated to 110°C).

The solubility of NH_4COONH_2 in liquid NH_3 is assumed to be very small even though literature data are not conclusive[27] and reports range from "highly soluble"[28] to completely insoluble.[29–31] No experimental study has investigated solubility of CO_2 in the parts per million by volume or parts per billion by volume range, which is of interest for the high-purity applications discussed in this study.

As cylinders are used to dryness and the pressure decreases as residual gas-phase NH_3 is withdrawn, strongly increasing free CO_2 concentrations are expected, assuming solid NH_4COONH_2 residuals are present. The decreasing NH_3 pressure results in an increase in CO_2 partial pressure as demanded by reaction equilibrium for the NH_4COONH_2 formation (Eq. 4). Additionally, the relative concentration of CO_2 increases as the overall pressure decreases according to Eq. 8. Estimated CO_2 concentrations as a liquid-dry cylinder is exhausted based on these calculations are shown in Fig. 9.

CO_2 REMOVAL FROM NH_3

Oxygenated impurities, such as CO_2, are detrimental to the performance of III/V semiconductor devices, and point-of-use purification, in addition to high-grade gas sources, are often implemented to optimize film growth processes. The complex thermodynamic behavior of CO_2 impurities in NH_3 opens questions about the requirements for purifier technologies for these applications. Because gas-phase CO_2 concentrations in NH_3 withdrawn from liquefied sources do not appear to exceed CO_2 levels of ~75 ppbv, independent of the total CO_2 content of the cylinder, CO_2 removal might not be necessary for less sensitive applications unless the liquid reservoir is exhausted. In case of high-purity requirements or if NH_3 is delivered from the liquid phase using total vaporization, state-of-the-art purifier materials are commercially available to reduce CO_2 contents by several orders of magnitude.

Point-of-use purifiers will also remove atmospheric impurities that are potentially introduced to the delivery system during cylinder change out. Residual CO_2 as an atmospheric contaminant might result in the formation of solid NH_4COONH_2 by reaction with NH_3 and deposit in the cylinder valve and line system. This NH_4COONH_2 residue will slowly decompose, potentially causing elevated CO_2 levels in the gas stream for extended time periods or enter the process tool in particulate form.

As an example for the efficiency of commercial technology, Fig. 10 shows the outlet concentration of a purifier based on a proprietary inorganic-adsorbent material (Nanochem NHX, 0.003-µm particle filter) challenged with 50-ppmv CO_2 in NH_3 using heated lines prior to entering the purifier. As CO_2 and NH_3 are mixed in heated lines but pass the unheated purifier inlet valves and purifier vessel, NH_4COONH_2 formation is expected to some degree in the unheated components. Both free CO_2 and NH_4COONH_2 particles suspended in the gas stream might then pass into the purifier.

Gas-phase CO_2 concentrations are below the detection limit of the GC-PDID at the purifier outlet, indicating removal efficiencies of at least three orders of magnitude at challenges in the parts-per-million by volume range. The mechanism for CO_2 removal from NH_3 is assumed to be a combination of CO_2 adsorption on the active sites of the purifier material and the formation and adsorption of NH_4COONH_2 in the presence of a high surface-area material.

Another benefit of the concentration threshold that is expected in gas-phase NH_3 withdrawn from liquefied sources is improved accuracy in the prediction of purifier lifetimes. Figure 11 shows a CO_2 capacity measurement performed with a Nanochem® NHX purifier at a 500-ppmv CO_2 challenge, resulting in a capacity of ~5.5 l CO_2/l purifier. The experiment was performed in He instead of NH_3 as measurements in NH_3 resulted in blockage of the purifier inlet with crystallized NH_4COONH_2. Sizing of purifier beds based on the measured capacity and predicted impurity calculated from the thermodynamic properties of CO_2 in NH_3 will be intrinsically more accurate than estimates for potentially strongly fluctuating impurities, such as H_2O.

CONCLUSIONS

The NH_3 gas delivered from cylinder sources may contain CO_2 in both free and chemically bound

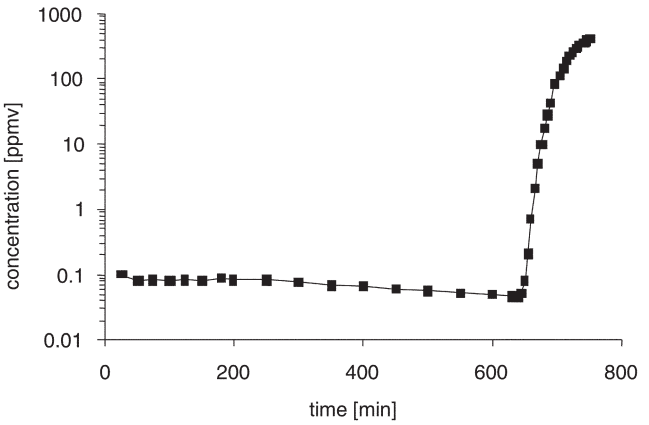

Fig. 11. Removal of 500-ppmv CO_2 from He by Nanochem® NHX purifier until breakthrough is reached (flow rate: 1 slpm, purifier volume: 60 cm^3).

forms at levels up to ~75 ppbv at ambient temperature. Higher concentrations can be expected if vaporized liquid sources are used close to depletion of the liquid phase or if the cylinder becomes liquid dry. If the sources are not used to complete dryness, CO_2 levels in the gas phase remain steady in accordance with the dissociation equilibrium, independent of the total amount of CO_2 present in the cylinder. Liquid concentrations are similarly based on the solubility of NH_4COONH_2 but excess solid NH_4COONH_2 might be sampled as particulates dispersed in the liquid stream, resulting in increased concentrations.

For high-purity applications where CO_2 is of potential concern, such as some microelectronic fabrication processes, point-of-use purification can remove both free and chemically bound CO_2 (as NH_4COONH_2) from an NH_3 gas stream.

REFERENCES

1. G. Parish, S. Keller, S.P. Denbaars, and U.K. Mishra, *J. Electron. Mater.* 29, 15 (2000).
2. G.A. Slack, L.J. Schowalter, D. Morelli, and J.A. Freitas Jr., *J. Cryst. Growth* 246, 287 (2002).
3. D.D. Koleske, A.E. Wickenden, R.L. Henry, and M.E. Twigg, *J. Cryst. Growth* 242, 55 (2002).
4. H. Kim, F.J. Fälth, and T.G. Andersson, *J. Electron. Mater.* 30, 1343 (2001).
5. J.A. Freitas Jr., W.J. Moore, B.V. Shanabrook, G.C.B. Braga, and S.K. Lee, *J. Cryst. Growth* 246, 307 (2002).
6. M. Hata, H. Takata, T. Yako, N. Fukuhara, T. Maeda, and Y. Uemura, *J. Cryst. Growth* 124, 427 (1992).
7. K.M. Coward, A.C. Jones, M.E. Pemble, S.A. Rushworth, L.M. Smith, and T. Martin, *J. Electron. Mater.* 29, 151 (2000).
8. L.M. Smith, S.A. Rushworth, M.S. Ravetz, R. Odedra, R. Kanjolia, C. Agert, F. Dimroth, U. Schubert, and A.W. Bett, *J. Cryst. Growth* 221, 86 (2000).
9. C.C. Allgood, *Solid State Technol.* 42, 63 (1999).
10. H.H. Funke, M.W. Raynor, B. Yucelen, and V.H. Houlding, *J. Electron. Mater.* 30, 1438 (2001).
11. M. Raynor, D. Sims, H. Funke, T. Watanabe, D. Fraenkel, J. Vininski, R. Torres, V. Houlding, and M. Owens, *Proc. CS-Max 2001*, Boston, MA, 9–11 July 2001.
12. D.A. Rodgers and F. Porter, U.S. patent 2,214,068 (10 September 1940).
13. L.J. Bagnell, A.M. Hodges, M. Linton, and A.W.-H. Mau, *Aus. J. Chem.* 42, 1819 (1989).
14. M.A. Isla, H.A. Irazoqui, and C.M. Genoud, *Ind. Eng. Chem. Res.* 32, 2662 (1993).
15. N.W. Krase and V.L. Gaddy, *J. Ind. Eng. Chem.* 14, 611 (1922).
16. I. Mavrovic, A.R. Shirley Jr., and G.R. Coleman, in *Kirk-Othmer Encyclopedia of Chemical Technology*, ed. J.I. Kroschwitz (New York: Wiley & Sons, 1998), 4th edition supplement, pp. 597–621.
17. D. Koschel, ed., *Gmelins Handbuch der Anorganischen Chemie* (Weinheim, Germany: Verlag, 1971), 8th edition, vol. 14(DI), pp. 391–396.
18. S. Inoue, K. Kanai, and E. Otsuka, *Bull. Chem. Soc. Jpn.* 45, 1339 (1972).
19. M. Raynor, D. Sims, J. Welchhans, R. Kubicek, T. Watanabe, R. Torres, and V.H. Houlding, *Proc. SEMICON West 2002*, San Francisco, CA, 22–24 July 2002.
20. T.J. Bzik, G.H. Smudde Jr., D.A. Zatko, and J.V. Martinez de Pinillos, in *Specialty Gas Analysis - A Practical Guide Book*, ed. J.D. Hogan (New York: Wiley-VCH, 1996), p. 163.
21. G.L. Long and J.D. Winefordner, *Anal. Chem.* 55, 712A (1983).
22. V.A. Lishnevskii and T.A. Madzievskaya, *Russ. J. Phys. Chem.* 56, 1342 (1982).
23. V.A. Lishnevskii, T.A. Madzievskaya, and M.I. Konyushko, *Russ. J. Phys. Chem.* 61, 36 (1987).
24. B.R. Ramachandran, A.M. Halpern, and E.D. Glendening, *J. Phys. Chem. A* 102, 3934 (1998).
25. R.N. Bennett, P.D. Ritchie, D. Roxburgh, and J. Thomson, *Trans. Faraday Soc.* 49, 925 (1953).
26. D. Janjic, *Helvetica Chimica Acta* 47, 1879 (1964).
27. R.W. Parry and S.G. Shore, *J. Am. Chem. Soc.* 80, 15 (1958).
28. A.F. Clifford and M. Gimenez-Huguet, *J. Am. Chem. Soc.* 82, 1024 (1960).
29. G. Fauser, U.S. patent 3,378,585 (16 April 1968).
30. M. Hirano and M. Tsunoda, U.S. patent 2,807,574 (24 September 1957).
31. W. Heitmann, U.S. patent 5,427,759 (27 June 1995).